J. Nano- Electron. Phys.
2 (2010) No3, P. 36-47

PACS number: 52.20.Hv, 52.65.Pp, 68.55. – a, 81.15.Cd

INFLUENCE OF ENERGY AVERAGING OF SPUTTERED ATOMS ON QUASI-EQUILIBRIUM STEADY-STATE CONDENSATION

A.A. Mokrenko, V.I. Perekrestov, Yu.O. Kosminska

Sumy State University,
2, Rimsky-Korsakov Str., 40007 Sumy, Ukraine
E-mail: perv@phe.sumdu.edu.ua

In this paper it is shown, that result of the quasi-equilibrium condensation in accumulative plasma-condensate system depends on the stability of the technological process, which in the general case is determined by the steadiness of the supersaturation, morphology and crystallographic structure of the growth surface, and also by the energy dispersion of sputtered atoms. The effect of energy averaging of sputtered atoms moving in high-pressure plasma has been established using the Monte-Carlo simulation. Results of the experimental investigation of the aluminum condensate formation near the thermodynamic equilibrium have shown that the increase in the working gas pressure more than 2,4 *Pa leads to the decrease in the film dispersity. This fact confirms the stability of the process.*

Keywords: *QUASI-EQUILIBRIUM CONDENSATION, PLASMA, THERMODYNAMIC EQUILIBRIUM, MAGNETRON SPUTTERING, SUPERSATURATION.*

(Received 14 July 2010, in final form 23 September 2010)

1. INTRODUCTION

Efficiency of nanotechnologies connected with the condensed state transition depends on the solution of two base problems. The first of them is defined by the creation of technological conditions, when phase transition occurs near thermodynamic equilibrium. Solution of the second problem is determined by the fact that quasi-equilibrium condensation should be in the steady-state conditions. It is necessary to emphasize that as condensation tends to the conditions of thermodynamic equilibrium, solution of the second problem becomes more complicated.

Consider the physical processes, which define stability of quasi-equilibrium condensation in plasma-condensate system under the condition that the substrate is placed on the cathode surface. Difference in the chemical potentials $\Delta\mu$ for atoms near the growth surface and those in the condensed state is the driving force of the condensation process. In the vicinity of thermodynamic equilibrium $\Delta\mu$ can be represented as a sum of three terms

$$\Delta\mu = \Delta\mu_s + \Delta\mu_e + \Delta\mu_r. \quad (1)$$

Here the first term depends on the pressure of precipitable vapor P. In the vicinity of the equilibrium [1]

$$\Delta\mu_s = (\Omega_v - \Omega_c)(P - P_e). \quad (2)$$

Here Ω_v and Ω_c are the specific volumes per one particle in vapor and condensate, respectively; P_e is the equilibrium vapor pressure, which in accordance with [2] can be written as

$$P_e = A(T)\exp\left(-\frac{E_d}{k_B T}\right). \quad (3)$$

Here k_B is the Boltzmann constant; $A(T) = \exp(\alpha T + \beta/T + \gamma)$, α, β, and γ are the constants characterizing the substance; E_d is the atom desorption energy. We note that in plasma-condensate system desorption energy takes an effective value [3-5]

$$E_d = E_{dv} - \Delta E, \quad (4)$$

where E_{dv} is the adatom desorption energy in the vapor-condensate system; ΔE is the accidental deduction characterized by the average value $\Delta \equiv \langle \Delta E \rangle$ and dispersion $\sigma \equiv \sqrt{\left\langle (\Delta E - \Delta)^2 \right\rangle}$. Presented above reduction of the desorption energy to the effective value due to the deduction of ΔE is defined by two factors. The first one is conditioned by incomplete thermal accommodation of adatoms, the energy of which in the moment of impact on the growth surface possesses higher values [2, 3]. The second factor is defined by direct energy transmission from plasma particles to adatoms. Obviously, in both cases dispersion σ is determined by the energy spread of plasma particles.

Physical meaning of the second term in correlation (1) is determined by the deviation of the growth surface temperature T from the equilibrium value T_e [1]

$$\Delta\mu_e = (s_v - s_c)(T - T_e). \quad (5)$$

Here s_v and s_c are the entropies of the vapor state and condensate.

The third term in correlation (1) is connected with the local changes of the difference in the chemical potentials due to the curvature and structural state of the growth surface [1, 6]. This term is determined based on the Herring relation [1, 7]

$$\Delta\mu_r = \frac{\Omega}{R_1}\left(\alpha + \frac{\partial^2\alpha}{\partial\beta_1^2}\right) + \frac{\Omega}{R_2}\left(\alpha + \frac{\partial^2\alpha}{\partial\beta_2^2}\right), \quad (6)$$

where R_1, R_2, β_1, and β_2 are the main radiuses of curvature and the corresponding angles determining changes in the surface energy α [1, 7].

In actual fact, $\frac{\partial^2\alpha}{\partial\beta_1^2}$ and $\frac{\partial^2\alpha}{\partial\beta_2^2}$ characterize changes in the structural state of a local area of the growth surface. It is also necessary to note that deviation of pressure from the equilibrium value $\Delta P = P - P_e$ can act as the absolute supersaturation.

Analyzing the terms in correlation (1) it is possible to establish three stability levels of quasi-equilibrium condensation. The first one is related to the case of the flat and isotropic with respect to the temperature and structure growth surface. Obviously, such type of the growth surface excludes the Gibbs-

Thomson effect from the process of the structure formation, i.e., $\Delta\mu_r = 0$. Constancy of the extremely weak pressure and temperature deviations from the equilibrium values can be the stability criterion in this case. For such simplified type of the growth surface pinning of adatoms will occur with equal probability in all its points.

The second stability level is related to the growth surface, which contains local areas of curvature and other structural non-uniformities. In this case condensation from plasma is accompanied by continuous changes of the structure and morphology characteristics in local areas of the growth surface [7], and factors, which influence these changes, are intricately interdependent. For example, curvature of the growth surface and the corresponding manifestation of the Gibbs-Thomson effect will influence the structural state of local areas of the growth surface. At the same time, in the vicinity of prominent parts of the growth surface, which in our case simultaneously is the cathode surface, fluctuations of the electric field intensity are possible. In virtue of these circumstances, focusing of precipitable ion fluxes on prominent parts of the growth surface is possible, and this is the prerequisite of the local changes of absolute supersaturation and temperature. Constancy of the averaged difference in the chemical potentials $\Delta\mu$ can be the stability criterion for such type of the growth surface. In particular case of the layer crystal growth on isotropic with respect to the temperature growth surface and the extremely weak manifestation of the Gibbs-Thomson effect, stability of the condensation process will be determined by the time-constancy of the critical energy E_c, which can be obtained based on correlation [5]

$$E_c = k_B T \ln\left[\frac{A(T)}{P_e}\right]. \qquad (7)$$

The third stability level is defined by the changes with time of the condensation kinetics in local points of the growth surface via the influence on these points of plasma particles with different energies and energy spread of condensable atoms. In accordance with (4), stability increase in this case can be expected at minimization of dispersion σ (see correlation (4)) or energy averaging of sputtered atoms under their displacement in plasma.

Taking into account the foregoing, two problems are solved in the present work. In the first one, by the simulation technique we study the energy averaging of sputtered atoms subject to the number of their interactions with plasma particles for different values of plasma pressure. In the final part of the work we represent the results of quasi-equilibrium condensation of Al subject to the energy averaging rate of plasma particles.

2. MODELING OF THE PROCESS OF ENERGY AVERAGING OF SPUTTERED ATOMS UNDER THEIR INTERACTION WITH THE WORKING GAS ATOMS

In accordance with [8], different density and energy of particles correspond to the different plasma types. In particular, for magnetron gas discharge plasma density can be within the range of 10^{17}-10^{19} м$^{-3}$. And in this case the following assumption is quite acceptable: all plasma particles are in thermodynamic equilibrium and, as a result, temperatures of electrons and ions in plasma are equal [8, 9]. Considering gas to be sufficiently rarefied, we

can neglect double, triple, fourfold, etc. atom collisions and suppose that only interactions, where collisions occur only between two plasma particles, take place. Consequently, interaction between atoms occurs only when they are very close to each other, i.e., they almost collide. For such model the perfect gas law [10] is applicable, starting from which

$$P_g = nk_B T_g, \tag{8}$$

where P_g is the total pressure produced by the sputtered and working gas atoms; $n = n_{Ar} + n_{Me}$ is the density of relatively heavy plasma particles; n_{Ar} is the concentration of argon atoms; n_{Me} is the concentration of sputtered atoms; T_g is the plasma temperature.

Mean free path λ for plasma particles is determined by the expression [9]

$$\lambda = 1 \Big/ \left(\sqrt{2} n \sigma_r \right), \tag{9}$$

where σ_r is the general cross-section, which takes into account the interaction cross-sections and pulse exchange between colliding particles, excitation and ionization processes.

It is necessary to note that effective cross-section is also the energy function of interacting particles (Fig. 1). Thus, it is shown in the work [11] that for average energies of interacting particles 2, 20, and 100 eV σ_r takes values $60 \cdot 10^{-20}$, $45 \cdot 10^{-20}$, and $38 \cdot 10^{-20}$ м^2, respectively. Taking into account correlation (8) and the value of σ_r for different energies of interacting particles, we have calculated dependences of the mean free paths λ on the argon plasma pressure. As it follows from the corresponding graphs (Fig. 1), decrease in the mean free path substantially slows down for pressures above 2,5 Pa.

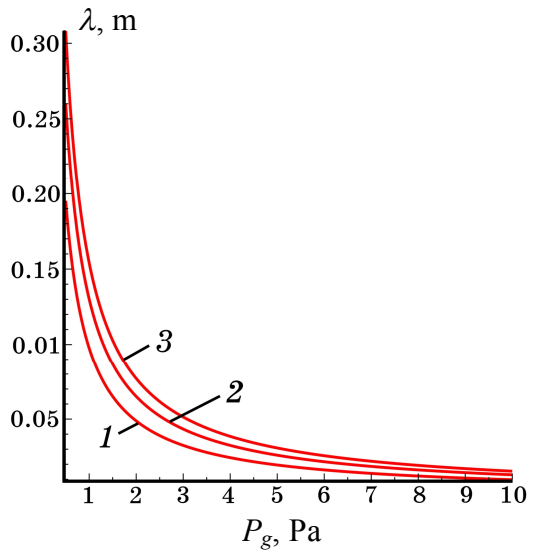

Fig. 1 *– Mean free path in Ar plasma at different atom energies. Energy, eV: 1 – 2, 2 – 20, 3 – 100*

Model approximations stated in the present section relate to the matter of evolution of the energy distribution of sputtered atoms under their interaction with plasma particles composed of the working gas atoms and sputtered substance. It is assumed here that the process is stationary and system parameters are time-independent. In this case we can apply statistical description of plasma particles by the energy distribution function $f(E)$ [10], which, as a matter of fact, is the consequence of the Maxwell velocity distribution and can be represented in the form

$$f(E) = 4\sqrt{\frac{2E}{\pi}}\left(\frac{n}{2P_g}\right)^{3/2}\exp\left(-\frac{nE}{P_g}\right). \tag{10}$$

A motion process of sputtered atoms at increased working gas pressures is of a particular interest from the point of view of fundamental investigations. Usually the primary energy spectrum of sputtered atoms is substantially wider [11-13] than the energy spectrum of plasma particles. Thus, in calculations we used primary energies of sputtered atoms up to 30 eV. In the first approximation the initial energy spectrum of sputtered atoms is described by the Sigmund-Thompson distribution [11, 14, 15]

$$f(E_r) = 2E_s\frac{E_r}{\left(E_r + E_s\right)^3}. \tag{11}$$

Here E_r is the initial energy of sputtered atoms; E_s is the binding energy of atoms with target surface. It is necessary to emphasize that distribution (11) approximately corresponds to the experimental results [11, 12]. In this case, the moving sputtered atoms experience numerous collisions with plasma particles that finally leads to their thermalization. A number of collisions of an atom with plasma particles N_0 determined by the relation [16]

$$N_0 \le 8m_k/m_a \tag{12}$$

(where m_k and m_a are the masses of sputtered material and working gas atoms, respectively) is the criterion of total thermalization or atom transition to the diffusive mode of motion. In the case of Al sputtering N_0 is approximately equal to 7.

In our case a low-temperature plasma where concentration of gas atoms essentially exceeds concentration of sputtered atoms is considered; and while calculating we used correlation $n_{Ar}/n_{Me} = 100$.

Under consideration of atom collisions, starting from the energy and momentum conservation laws, correlation for the sputtered atom energy before E_k and after E_k' collision is determined by the expression [16]

$$E_k' = 2\left(\sqrt{\mu_k} + 1/\sqrt{\mu_k}\right)^{-2}\left\{E_k\left(\mu_k + 1/\sqrt{\mu_k}\right)\ /2 + E_a + \sqrt{E_kE_a}\left(\sqrt{\mu_k} + 1/\sqrt{\mu_k}\right)\cos\phi_0 + \right.$$
$$\cos\chi\left[\left(E_k\ /\sqrt{\mu_k} + E_a\sqrt{\mu_k} - 2\sqrt{E_kE_a}\cos\phi_0\right)\times\right.$$
$$\left.\left.\times\left(E_k\sqrt{\mu_k} + E_a\ /\sqrt{\mu_k} + 2\sqrt{E_kE_a}\cos\phi_0\right)\right]^{1/2}\right\}, \tag{13}$$

where $\mu_k = m_k/m_a$; ϕ_v is the random angle between the velocity directions of metal and gas atoms.

To define the scattering angle χ at collision of two particles, it is necessary to take into account the influence of the interaction potential $u(r)$. In our case, for the description of interaction between sputtered and gas atoms the Lennard-Jones potential was used

$$u(r) = 4\varepsilon\left[\left(r_0/r\right)^{12} - \left(r_0/r\right)^6\right], \tag{14}$$

where ε is the potential well depth; r is the interparticle spacing; r_0 is the coordinate of the equilibrium state of atoms.

In the energy range $10 < E/\varepsilon < 10^4$, which we are interested in, the approximation formula for determination of $\cos\chi$ can be written as

$$\cos\chi \approx 1 - 2\left[1 - \left(\rho_{np}/r_0\right)^2 0.5537(E/\varepsilon)^{0.1406}\right]^{1.8834(E/\varepsilon)^{0.0286}}. \tag{15}$$

Based on the Monte-Carlo method, using the random quantities such as the collision angle and plasma particle energy and taking into account correlations (10)-(15), the block-diagram of the calculation of the energy distribution of sputtered atoms depending on the number of atom collisions with plasma particles is created (Fig. 2).

Calculation data has confirmed the validity of the assumption that after interaction of sputtered atoms with heavy plasma particles the atom thermalization occurs. This is exhibited in the narrowing of the energy spectrum of sputtered particles (Fig. 3) and the corresponding decrease in dispersion σ that is an important factor of the stability increase in the quasi-equilibrium condensation. In this case after total thermalization of sputtered atoms their motion can be described by the diffusion equations.

3. PROCEDURE OF QUASI-EQUILIBRIUM CONDENSATION OF ALUMINUM

Currently, in the widespread techniques, at the best, stability of quasi-equilibrium condensation is kept up using the feedback between the structure formation kinetics and parameter control system [17]. Since it is difficult to track on-line the formation kinetics of low-dimension systems, realization of the stationary conditions of the process is the intractable problem. Therefore, we have proposed the technological approach, the basis of which is the self-organization of time-independent critically small relative supersaturations. Such self-organization can be realized based on the accumulative plasma-condensate system [5, 18], which consists of the magnetron planar atomizer and associated hollow cathode (Fig. 4). Physical operation principles of such systems and mathematical model of self-organization of critically small relative supersaturations are stated in detail in [5, 18]. It is necessary to emphasize that when using the accumulative plasma-condensate systems and isotropic with respect to the structure and temperature growth surface, one can study the influence of the third stability level on the structure formation mechanisms.

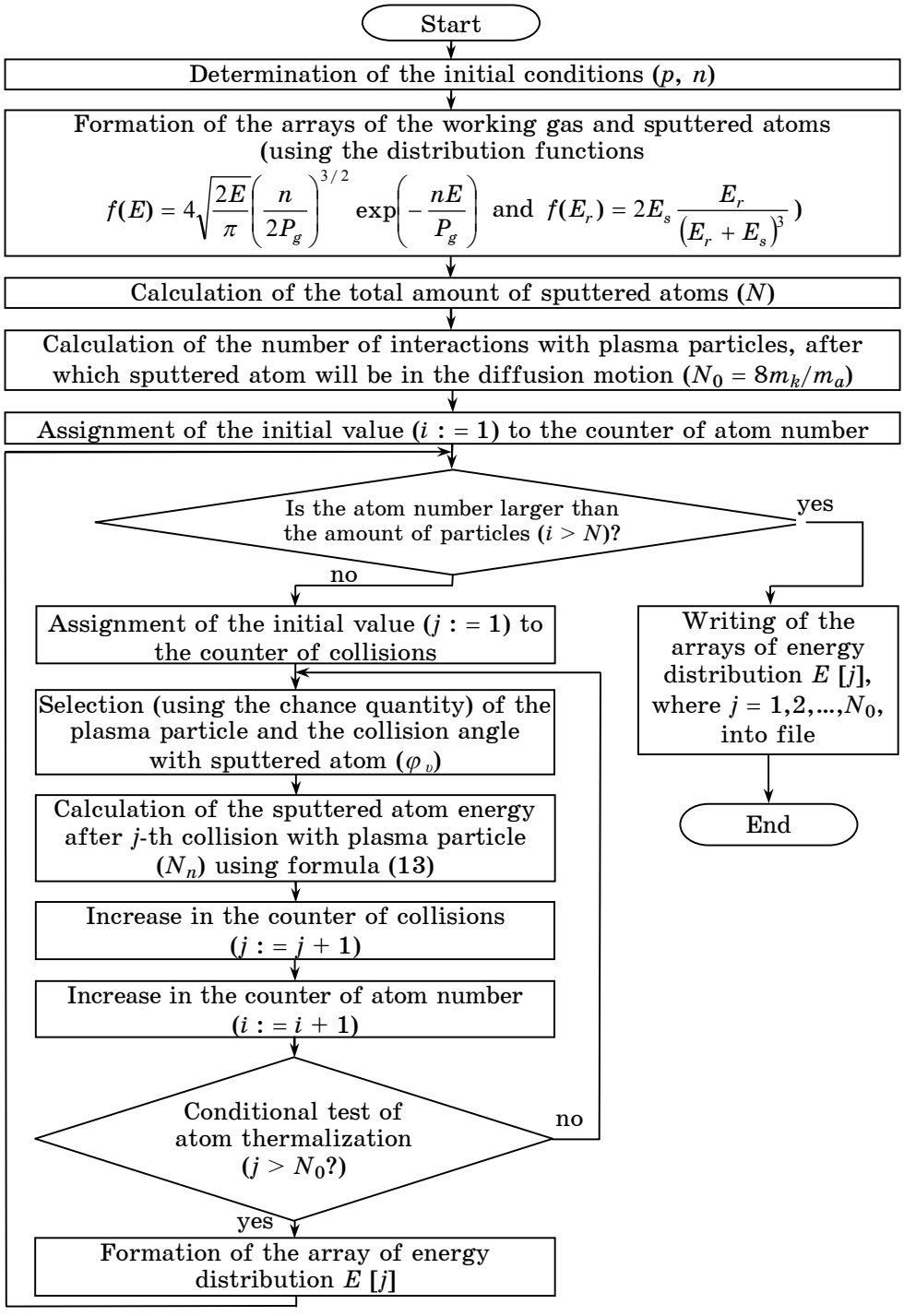

Fig. 2 *– Calculation block-diagram of the energy distribution of sputtered atoms*

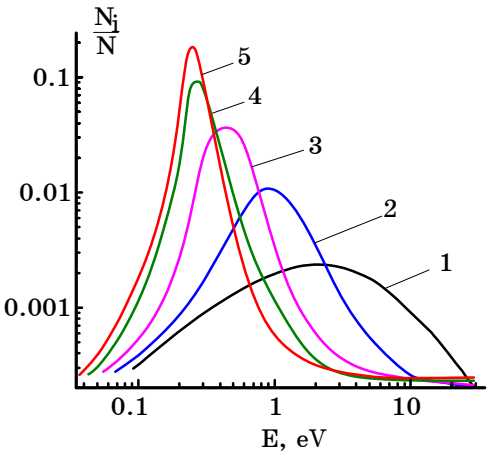

Fig. 3 *– Energy distributions of sputtered atoms after interaction with plasma particles at* 10 *Pa: 1 – initial distribution; 2-5 – distributions after interaction with plasma (2, 4, 7, and 13 collisions of sputtered atom with plasma particles, respectively)*

The necessary purity of the working gas, in the capacity of which argon was used, was achieved due to the long-term (~ 30 hours) sputtering and the subsequent titanium condensation on the internal walls of the working chamber [19]. Argon purification did not cease during the whole technological process, and this allowed to create the conditions of aluminum condensation, when the partial pressure of all reactive gases was ~ 10^{-7}-8 10^{-8} Pa.

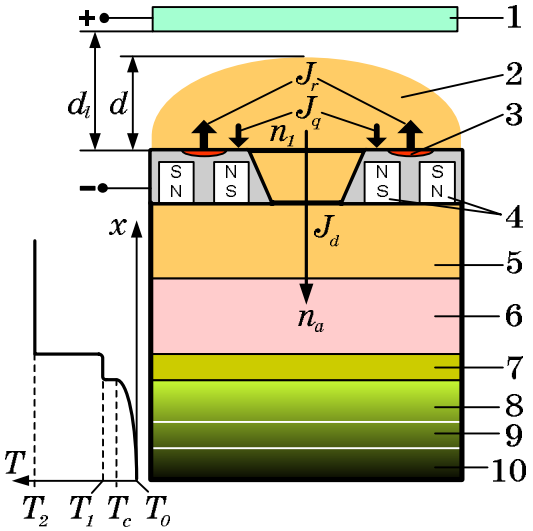

Fig. 4 *– Cross-section of the axially symmetric accumulative plasma-condensate system (1 – anode; 2 – thermalization region of sputtered atoms; 3 – erosion zone; 4 – system of magnets; 5 – hollow cathode; 6 – region of the annular mass transfer; 7 – layer of adatoms; 8 – condensate; 9 – substrate; 10 – cooler). Qualitative temperature distribution near the growth surface is represented on the left*

Aluminum condensation was performed on the KCl (001) cleavage faces. In the conditions of quasi-equilibrium condensation, defects and morphology inhomogeneities of the substrate can become the preferable active centers of atom pinning. In this connection we have to note that anion vacancies of Cl^- formed under the crystal bombardment by the charged particles [3, 7, 20, 21] possess high activity on (100) of alkali halide crystal. In our case the developed system of such defects was formed on the first stage of the sputtering system operation, which was accompanied by plasma irradiation of KCl (001). Evaluation of the condensate thickness was carried out under the discontinuity and folding of condensates directly in TEM, and the discharge power was 5,8 Вт.

4. EXPERIMENTAL RESULTS AND DISCUSSION

At first we consider the structure formation mechanism of Al condensates at relatively low working gas pressures (P_{Ar} = 1 Pa), i.e., at higher values of dispersion σ. Based on the TEM and electron diffraction it was established that the initiation process occurs uniformly all over the whole surface in the absence of nucleation of separate supercritical nucleuses and their further coalescence (Fig. 5a). Here we should pay attention to the fact of the nanocrystalline structure formation (Fig. 5a), in which recrystallization processes under the heating by an intensive electron beam are not observed. Such investigations were performed directly in the electron microscope, and to increase the intensity of an electron beam condenser aperture was removed. Consequently, such type of the growth surface possesses isotropic with respect to the temperature and structure characteristics that allows to reveal the influence of the third stability level on the structure formation mechanism.

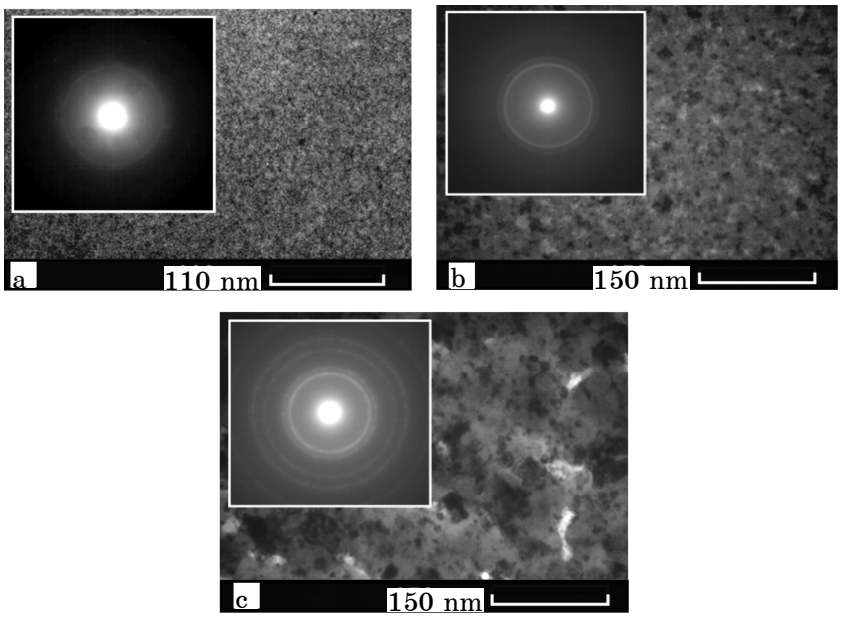

Fig. 5 *– Initial stage of initiation and growth of the condensate at* P_w = 5,8 *W and* P_{Ar} = 1,4 *Pa. Deposition time, s: a* – 60*; b* – 150*; c* – 300

Structure analysis on the subsequent growth stages (Fig. 5b, c) implies that with the increase in the layer thickness approximately up to 150 nm the gradual decrease in the condensate dispersity occurs. Seemingly, such specificity of the condensate initiation and growth is conditioned by the fact that in the extreme case of critically small supersaturations the substance condensation is confined by the only possible type of atom-by-atom pinning of adatoms on the anion vacancies of KCl. The difference is that in last two variants, as a rule, the atomic-smooth surface of mono-crystalline substrate with minimum amount of point defects is used, and in our case under the action of plasma on KCl (001) the so significant density of Cl^- vacancies is formed, that, in actual fact, this surface is transformed to the atomic-rough one. In turn, rigid atom-by-atom pinning on the atomic-rough surface also leads to the formation of new-formed atomic-rough growth surface due to the difference between KCl and Al lattice parameters.

Sequence of repetitive stages of such atom-by-atom building is not practically studied up to now and is of significant interest from the scientific and practical points of view. Obviously, the possibility of the transition to the more structurally equilibrium form appears with the increase in the condensate thickness that is expressed in a gradual increase in the grain size.

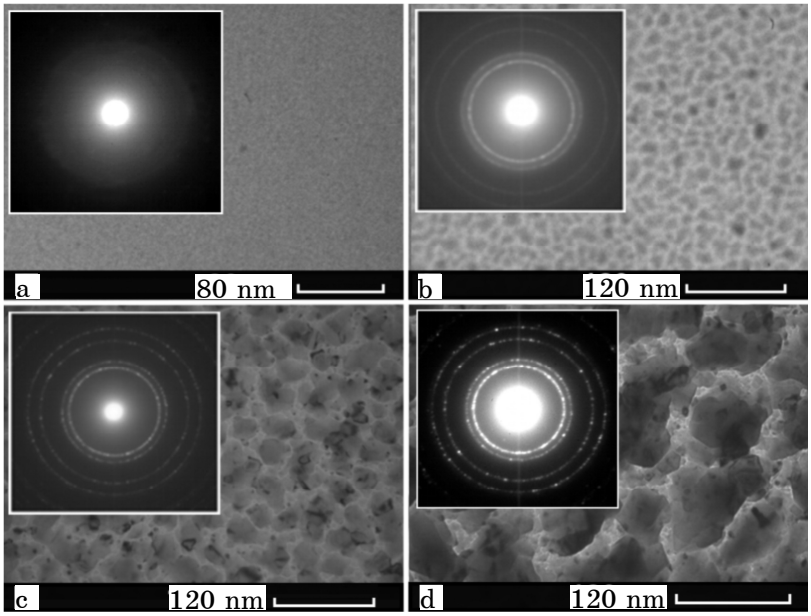

Fig. 6 *– Initial stage of initiation and growth of the condensate at* P_w = 5,8 *W and* P_{Ar} = 3 *Pa. Deposition time, s: a* – 60*; b* – 80*; c* – 150, *d* – 300

Increase in P_{Ar} more than 2,5 Pa violates the transition smoothness from the highly dispersed basic layer to the relatively large-grained polycrystal. In this case at the thickness of nanocrystalline basic layer of ~ 8-15 nm the homonucleation and high-speed growth of the relatively large crystals occurs (Fig. 6). Seemingly, the relatively sharper transition is conditioned by the increased structural non-equilibrium of the basic layer that is the result of the energy averaging of plasma particles or increase in the technological process stability.

Sufficiently long-term condensation (~ 2 hours) at P_{Ar} more than 2,5 Pa leads to the growth of separate relatively coarse faceted crystals (Fig. 7).

Such layer growth of the crystals is possible only at increased working gas pressures, i.e., at high stability of the condensation process of all levels.

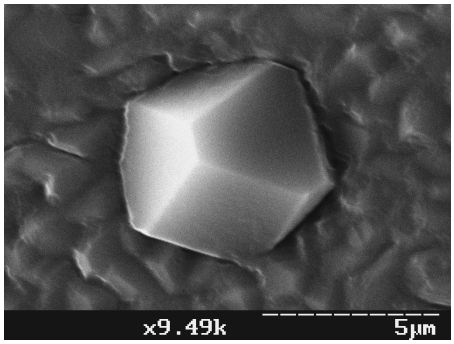

Fig. 7 – *Surface image of the Al condensate obtained using the scanning electron microscope*

5. CONCLUSIONS

Result of quasi-equilibrium condensation in plasma-condensate system depends on the technological process stability, which in the general case is determined by the constancy of supersaturation, structure and morphology characteristics of the growth surface, and the energy spread of condensable atoms as well. Based on the model approximations we have confirmed the fact of the narrowing of energy spectrum of sputtered atoms as a result of their interaction with plasma particles that is the prerequisite for the increase in the stability of quasi-equilibrium condensation.

As the experimental results have showed, increase in the stability of quasi-equilibrium condensation leads to the decrease in the dispersity of Al condensates, and layer growth of separate relatively coarse crystals as well. Thereby, we have experimentally confirmed high stability of the condensation process at the working gas pressures exceeding 2,5 Pa.

REFERENCES

1. A.A. Chernov, E.I. Givargizov, Kh.S. Bagdasarov, V.A. Kuznetsov, L.M. Dem'yanets, et al., *Sovremennaya kristallografiya. Obrazovanie kristallov. T.3* (M.: Nauka: 1980).
2. L.I. Maissel, R. Glang, *Handbook of Thin Film Technology* (New York: McGraw-Hill: 1970).
3. V.I. Perekrestov, A.S. Kornyushchenko, Yu.A. Kosminskaya, *Phys. Solid State* **50**, 1357 (2008).
4. F.O. Goodman, *Phys. Chem. Solids* **23**, 1269 (1962).
5. V.I. Perekrestov, A.I. Olemskoi, Yu.O. Kosminska, A.A. Mokrenko, *Phys. Lett. A* **373**, 3386 (2009).
6. Guozhong Ca, *Nanostructures & nanomaterials* (London: Imperial College Press, 2004).
7. V.I. Perekrestov, A.S. Kornyushchenko, Yu.A. Kosminskaya, *JETP Lett.* **86**, 767 (2007).
8. L.A. Artsimovich, R.Z. Sagdeev, *Fizika plazmy dlya fizikov* (M.: Atomizdat: 1979).

9. P.M. Martin, *Handbook of Deposition Technologies for Films and Coatings* (Science: Applications and Technology Elsevier: 2005).
10. L.D. Landau, E.M. Lifshitz, *Teoreticheskaya fizika. T.5. Statisticheskaya fizika* (M.: Nauka: 1976).
11. M.W. Thompson, *Vacuum* **66**, 99 (2002).
12. A.V. Phelps, *J. Phys. Chem. Ref. Data* **20**, 557 (1991).
13. W.D. Davis, T.A. Vanderslice, *Phys. Rev.* **131**, 219 (1963).
14. S.N. Sambandam, S. Bhansali, V.R. Bhethanabotla, D.K. Sood, *Vacuum* **80**, 406 (2006).
15. S. Senthil Nathan, G. Mohan Rao, S. Mohan, *J. Appl. Phys.* **84**, 564 (1998).
16. A.G. Zhiglinskiy, *Massoperenos pri vzaimodeistvii plazmy s poverhnost'yu* (M.: Energoatomizdat: 1991).
17. R.F.C. Farrow, *Molecular beam epitaxy: applications to key materials* (Noyes Publications: New Jersey: 1995).
18. V.I. Perekrestov, A.I. Olemskoi, A.S. Kornyushchenko, Yu.A. Kosminskaya, *Phys. Solid State* **51**, 1060 (2009).
19. V.I. Perekrestov, S.N. Kravchenko, *Instrum. Exp. Tech.* **45**, 404 (2002).
20. V.I. Perekrestov, A.V. Koropov, S.N. Kravchenko, *Phys. Solid State* **44**, 1181 (2002).
21. V.I. Perekrestov, *Tech. Phys. Lett.* **31**, 830 (2005).